Analytica Chimica Acta 1086 (2019) 110–115

Contents lists available at ScienceDirect

Analytica Chimica Acta

journal homepage: www.elsevier.com/locate/aca

A highly sensitive electrochemical sensor based on DNA Y-Junction for detection of estrogen receptor using target protein protection strategy

Jinlong Li [a, *, 1], Kai Hu [b, 1], Yongchen Zhang [a], Zhaoli Zhang [a], Yongfeng Yang [a, **]

[a] Department of Laboratory Medicine, the Second Hospital of Nanjing, Nanjing University of Chinese Medicine, Nanjing, 210003, PR China
[b] Department of ophthalmology, the Nanjing Drum Tower Hospital, the Affiliated Hospital of Nanjing University Medical School, Nanjing, 210004, PR China

HIGHLIGHTS

- An electrochemical method for Estrogen receptor (ER) detection has been developed.
- The DNAzyme-mediated signal amplification is based on the formation of DNA Y-Junction.
- DNA Y-Junction is modified by target protein protection strategy.
- The method shows a lower detection limit by the DNAzyme-mediated signal amplification.
- ER is detected effectively in cell samples.

GRAPHICAL ABSTRACT

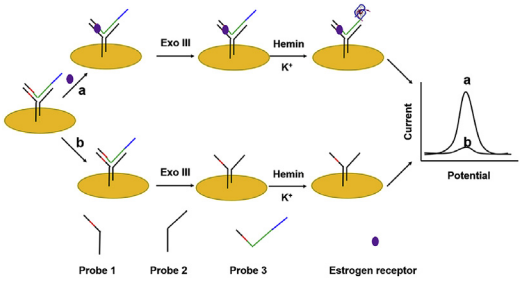

ARTICLE INFO

Article history:
Received 28 May 2019
Received in revised form
30 July 2019
Accepted 12 August 2019
Available online 17 August 2019

Keywords:
Estrogen receptor
DNA Y-Junction
Electrochemical sensor
Breast cancer
Biosensor

ABSTRACT

Estrogen receptors (ERs) play a major role in the signaling pathways and participate in regulating and maintaining the basic activities of life. The abnormal expression of ERs has a significant effect on tumorigenesis. Herein, we propose an electrochemical method for detecting ERs based on the formation of DNA Y-Junction with a 3′-blunt end. The DNA Y-junction was designed to have one of its arms bound to an ER. When an ER was bound to the junction, which was immobilized on the electrode surface, it protected the DNA Y-junction from Exo III-catalyzed digestion. DNA Y-Junction also contained G-quadruplex rich duplex, which generated electrochemical signals when hemin was added to the electrode, resulting in the quantitative detection of ERs. The detection range of the ER using this method was 0.1 −200 nM with a detection limit of 0.034 nM. Since this assay can be employed to detect ERs in tumor cells, it may be useful in tumor diagnosis in the future.

1. Introduction

Estrogen receptor (ER) is a member of the nuclear receptor superfamily, which can regulate the growth and differentiation of reproductive system and participate in the regulation of various physiological and pathological processes [1–4]. Emerging research suggest that ER is not only related to the tumorigenesis of estrogen target organs, such as breast cancer, ovarian cancer, and endometrial cancer, but are also widely expressed in non-target organs such as liver cancer, gastric cancer, lung cancer, and colorectal cancer [3,5–7]. Thus, it is a potential marker of various tumors. Therefore, detection of ER may provide an effective means for the early diagnosis of cancers.

* Corresponding author.
** Corresponding author.
E-mail addresses: lijinlong1028@126.com (J. Li), tangb_@126.com (Y. Yang).
[1] These authors contributed equally to this work.

https://doi.org/10.1016/j.aca.2019.08.028
0003-2670/

The conventional ER assays are mainly based on antibody-antigen specific reactions, such as immunohistochemistry assay [8], enzyme-linked immunosorbent assay (ELISA) [9], and western blotting assay [10]. However, these methods usually require expensive estrogen receptor antibodies, laborious operations, fluorescence probes, and special instruments, which hinder their application in resource-limiting settings. Compared to these methods, electrochemical biosensors possess superior features, such as good sensitivity, low-cost, simplicity, and portability, providing a promising platform for the highly accurate analysis of ER [11,12].

Herein, we have developed an electrochemical sensing platform for the detection of ER in tumor cells with high sensitivity by coupling DNAzyme-mediated signal amplification that is based on the formation of DNA Y-junction induced by the target protein protection strategy. DNA Y-junction consists of three DNA strands hybridized with one another, which provides better flexibility and repeatability with the capacity of anti-jamming for building biosensing platforms [13–16]. Compared with the existing methods, our strategy has the following advantages. First, using DNA based probes allows cost-efficient analysis as compared to the use of expensive antibodies [17–20]. Second, the technique is label free as compared the methods that require laborious labelling steps. Third, the simplicity of the electrochemical method ensures that it is easy to train personnel to use the method. Therefore, the proposed sensing system will be a promising candidate for ER detection in clinical diagnostics.

2. Experimental

2.1. Reagents and materials

Human recombinant ER was purchased from Invitrogen (Carlsbad, CA, USA). Exo III and NEB buffer I were obtained from New England Biolabs (Ipswich, WA, USA). Mercaptoethanol (MCH), RIPA buffer, hydroquinone (HQ) sulfuric acid, hydrogen peroxide (H_2O_2), hemin, EDTA, and tris (2-carboxyethyl) phosphine hydrochloride were purchased from Sigma-Aldrich. All the oligonucleotide sequences were synthesized by Shanghai Sangon Biotechnology Co. Ltd. (Shanghai, China) and stored in the TE buffer at −20 °C. The base sequences of the probe1 (P1), probe2 (P2), and probe3 (P3) are shown in Scheme 1 [12,21–23].

All other reagents were of analytical reagent grade and used as received. All the buffers were prepared with deionized water, which was purified with a Milli-Q purification system to a resistance of 18 MΩ cm.

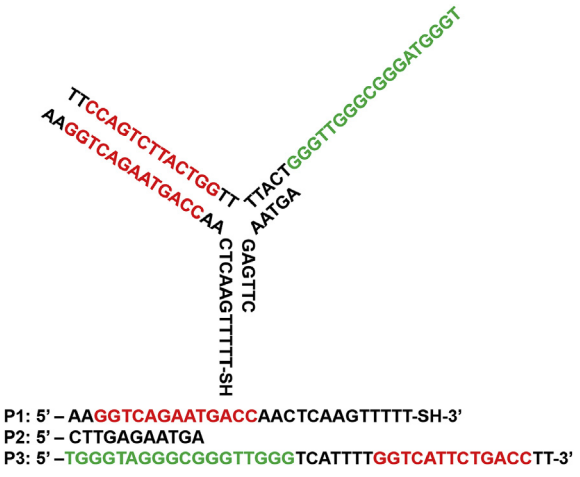

Scheme 1. The structure and sequence of probes.

2.2. Apparatus

CHI 660 E electrochemical workstation (CH Instrument, USA) was used for all the electrochemical measurements. The electrochemical system consisted of a working electrode, an auxiliary electrode (platinum wire), and a reference electrode.

2.3. Cell culture and ER extraction

MCF-7 cells were cultured in DMEM medium containing 10% fetal calf serum. All cells were harvested from adherent cell culture by RIPA buffer, followed by washing with cold PBS. The cells were incubated for 30 min on ice and then centrifuged at 12 000 rpm for 5 min at 4 °C. Finally, the supernatant was collected, which was flash frozen and stored at −80 °C before use.

2.4. Preparation of the biosensor

Gold electrode was treated with the following steps as reported in the previous literature [20,24,25]. 10 μL of DNA immobilization solution containing 0.2 μM of P1 was first added and the DNAs were self-assembled onto the gold electrode surface via gold-thiol chemistry for 12 h at 4 °C. To eliminate non-specific DNA adsorption and block the remaining nonspecific binding sites, the gold electrode was further treated with 1 mM MCH solution for 30 min and then rinsed with DNA hybridization buffer. Later, 10 μL of DNA hybridization buffer containing 1 μM of P3 (signal probe) and 1 μM of P2 were dropped onto the gold electrode surface for 2 h at 37 °C. After hybridization, the electrode was thoroughly rinsed with deionized water and used for the following experiments.

2.5. Electrochemical detection of ER

Electrochemical detection of ER was performed as follows: the DNA Y junction-modified gold electrode was immersed in 150 μL DNA-binding buffer solution containing ER or cell lysate for 30 min at 37 °C. Then, the electrode was thoroughly rinsed with PBS three times and immersed into 50 μL of NEB buffer I at 37 °C for 30 min, which contained 2 units of Exo III. Then, EDTA was added to a final concentration of 20 mM to terminate the Exo III reaction, the electrode was rinsed with PBS buffer and deionized water successively three times. 10 μL of freshly prepared hemin solution containing 25 mM HEPES, 100 μM hemin, 200 mM NaCl, 12.5 mM $MgCl_2$, and 50 mM KCl was dripped on to the electrode surface at 25 °C for 1 h. Because the DNA has many guanine-rich sequences of P3, G-quadruplex-based DNAzyme was formed. Then, the electrode was used for the following measurements.

2.6. Electrochemical measurements

Cyclic voltammogram (CV) and electrochemical impedance spectra (EIS) were determined in 5.0 mM of $[Fe(CN)_6]^{3-/4-}$ containing KCl (0.1 M) with the frequency in the range of 10^{-1} to 10^5 Hz. Differential pulse voltammetry (DPV) was performed in 5 mL of PBS (0.1 M, pH 7.4) containing 1.0 mM H_2O_2 and 0.2 mM HQ with the scan range from −0.2 to 0.2 V.

3. Results and discussion

3.1. Method design

The working principle of the designed electrochemical

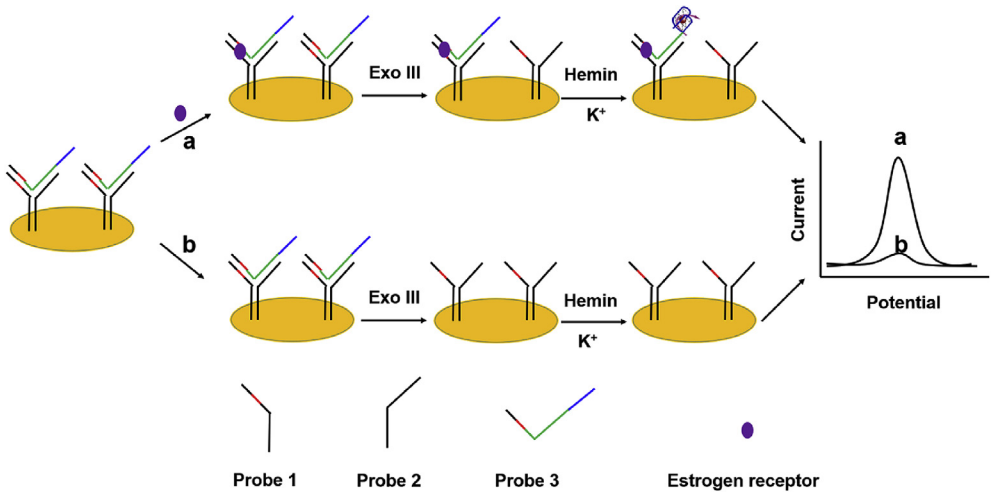

Scheme 2. Schematic illustration of the detection of ER.

biosensor for ER determination is illustrated in Scheme 2. P1 was modified on the gold electrode surface through Au–S bond. The P2 and P3 can hybridized with P1 incompletely. P3 consisted of G rich sequence and served as an electroactive signaling probe. Hybridization of P2 and P1 grafts the P3 strand onto the electrode surface, forming a stable Y junction with a 3′-blunt end at the signaling strand. In the presence of ER, which binds specifically to the double stranded region of P1–P3, this part of the DNA Y junction is protected from digestion when Exo III is introduced into the system. The G-rich region of the P3 forms HRP-mimicking DNAzyme after hemin is added into the system. Thus, a strong electrochemical signal is generated. Nevertheless, in the absence of ER, the Exo III can digest the double stranded P1–P3 and then liberate the G-rich region of the P3, resulting in no electrochemical signal.

3.2. Characterization of the modification process of the electrode

In order to confirm the successful preparation of the modified electrodes, EIS was performed on different modified electrodes in 0.1 M KCl containing 5.0 mM $[Fe(CN)_6]^{3-/4-}$ [26–28]. As shown in Fig. 1 A, EIS of the bare electrode was nearly a straight line (curve a). A relatively small Ret was obtained when P1 was modified on the gold electrode (curve b) and the magnitude of Ret increased after the modification of P2 and P3 because of the repulsion of $[Fe(CN)_6]^{3-/4-}$ by the negatively charged DNA monolayer on the electrode surface (curve c, and d). After binding to the ER, an increase in Ret was observed (curve e). After incubation with Exo III, the magnitude of Ret decreased (curve f). These results indicated the successful binding of ER leads to the increase of Ret. The modification process is further proved by Cyclic voltammogram (CV) [29,30]. CV curves of 5.0 mM $[Fe(CN)_6]^{3-/4-}$ redox probe in 0.1 M KCl solution with scan rate of 100 mV/s. As shown in Fig. 1 B, a biggest redox peak current is existed of bare electrode (curve a). The redox peak currents are decreased progressively after the step by step self-assembling of P1, P2, P3 and ER on the surface of bare electrode (curves b, c, d, and e). After incubation with Exo III, the redox peak current is increased to some extent (curve f), which are in accordance with that observed in EIS. Therefore, the above results prove the successful modification of the electrode surface.

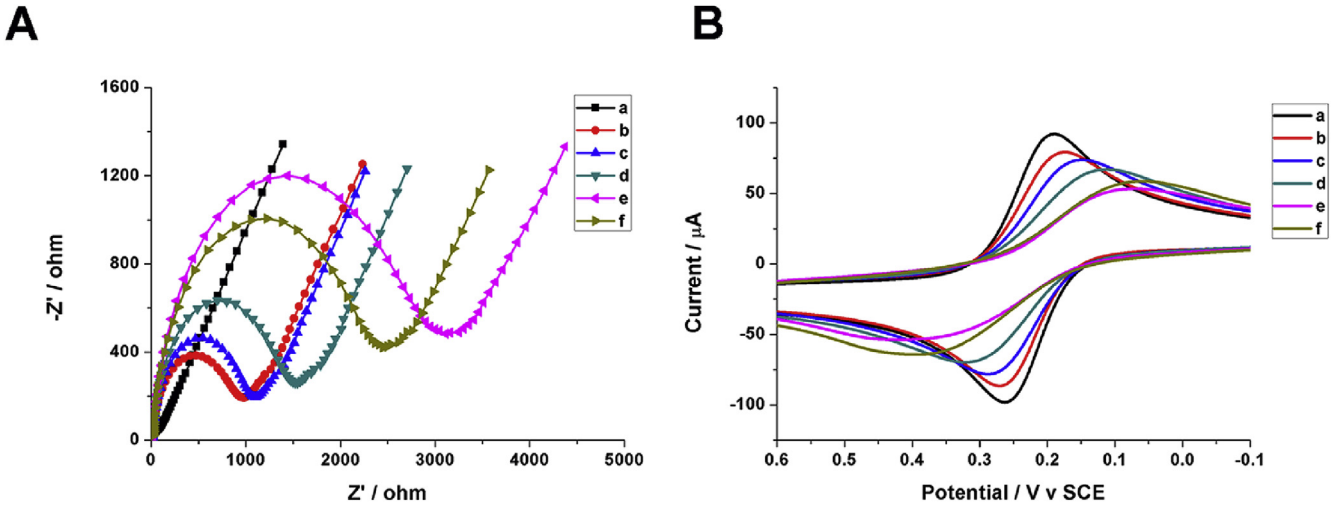

Fig. 1. (A) EIS and (B) CV measurements for different modified electrodes: (a) bare gold electrode, (b) above electrode after P1 modification, (c) above electrode after P2 modification, (d) above electrode after P3 modification, (e) above electrode after incubation with ER, (f) above electrode after incubation with Exo III. (For interpretation of the references to color in this figure legend, the reader is referred to the Web version of this article.)

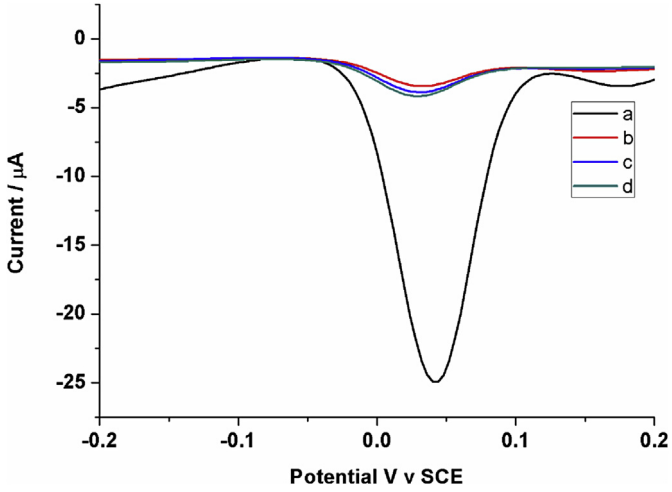

Fig. 2. DPV curves for gold electrode treated successively with (a) P1, P2, P3, ER, and Exo III, (b) P1, P2, P3, and Exo III, (c) P1, P2, ER, and Exo III, (d) P1, P3, ER, and Exo III, in 0.1 M PBS (pH 7.4) containing 1.0 mM H_2O_2 and 0.2 mM HQ. (For interpretation of the references to color in this figure legend, the reader is referred to the Web version of this article.)

3.3. The feasibility of the electrochemical method

DPV was selected to investigate the electrochemical behaviors of different electrodes from −0.2 to 0.2 V. As shown in Fig. 2, in the presence of ER, a significant current signal was observed, indicating that P3 was protected from Exo III digestion and formed HRP-mimicking DNAzyme when hemin was added on the gold electrode surface (curve a). However, in the absence of ER, only a mild current signal response was seen because P3 was digested by Exo III (curve b). Furthermore, in the absence of P3 (curve c) and P2 (curve d), only small electrochemical signals were observed, which clearly demonstrated that P2 and P3 were necessary to achieve significantly amplified signals. Therefore, the above results indicated the feasibility of this method for the detection of ER.

3.4. Optimization of the detection conditions

Experimental variables affecting the whole sensing process were optimized. Since the concentration and the reaction time of Exo III significantly influence the amplification reaction, the systems with different Exo III concentrations and different reaction time were investigated, respectively. As shown in Fig. S1A, when other conditions were kept unchanged, the peak current reached a minimum when 2 units Exo III was added to the reaction system. The above results showed that 2 units of Exo III was enough for the reaction system. Thus, 2 units of Exo III was chosen for the following experiments. As can be seen from Fig. S1B, the peak current decreased significantly with the Exo III incubation time from 10 min to 40 min. Then, the peak current attained thermal stability in 30 min. The result indicated that excessive incubation time might hinder electron transfer from benzoquinone to the electrode. Thus, 30 min was adopted as the optimal incubation time.

3.5. Electrochemical assay for ER determination

Under the optimum conditions, the detection for ER was investigated using DPV. As shown in Fig. 3 A, the DPV peak current increased with increasing ER concentration. A linear relationship between peak current and logarithm of the concentration of ER was plotted (Fig. 3 B) in the range of 0.1–200 nM. The calibration equation obtained from this curve was $y = -5.58\ x\ -11.8$ ($R^2 = 0.993$). The calculated limit of detection (LOD) was 0.034 nM (S/N = 3). The proposed label-free biosensor showed good sensitivity that was comparable to the existing methods, which not only decreased the background signal by preventing the labeling moieties from interfering with protein binding but also simplified the fabrication of the sensors (Table 1). As is indicated by the data and error bars in Fig. 3, the stability and repeatability of the method are satisfactory.

3.6. Selectivity of the biosensor

To characterize the specificity of the biosensor, we challenged the biosensor with other interfering proteins, such as BSA, AFP, CEA, CA125, CA153 and T4PNK. As shown in Fig. 4, high peak current was

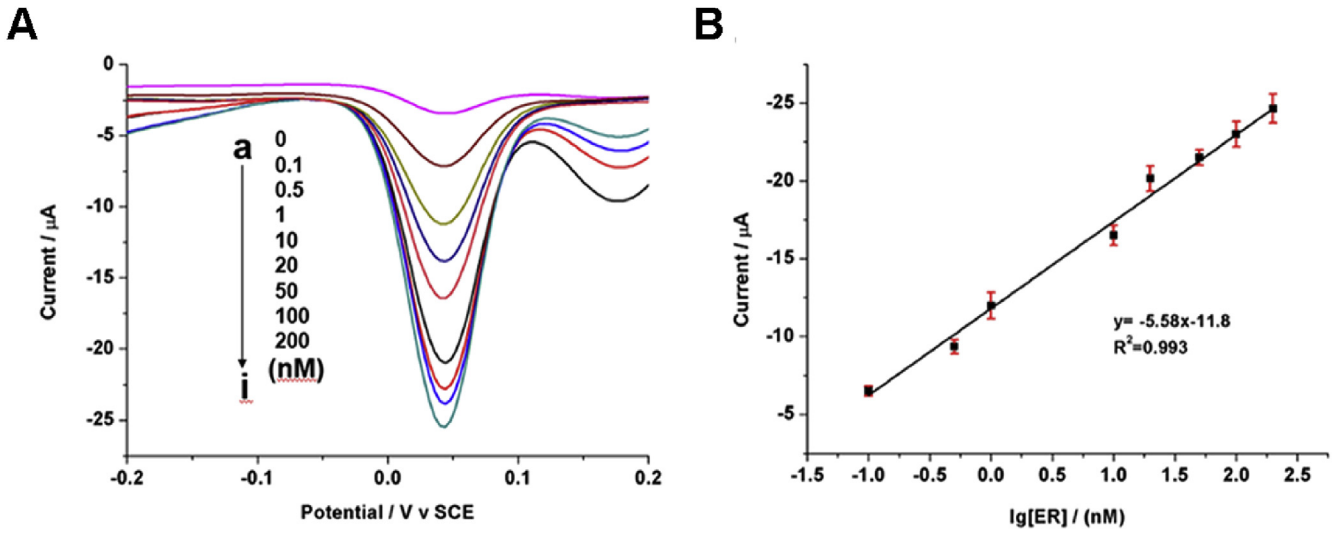

Fig. 3. (A) Differential pulse voltammetry (DPV) curves obtained at the modified electrodes to quantify ER. Curves a-i corresponding to ER concentrations of 0, 0.1, 0.5, 1, 10, 20, 50 100, and 200 nM. (B) The calibration curve of (A). Error bars indicate standard deviation of three independent experiments.

Table 1
Comparison of the detection performances of the present method with previously reported ones.

No.	Detection method	Linear range	Detection limit	Detection time	Reference
1	Electrochemical (DPV)	0.001–1000 pg/μL	0.001 pg/μL	80 min	[11]
2	Electrochemical (SWV)	0.5–100 nM	0.38 nM	31 min	[12]
3a	Electrochemical (DPV)	0.1–200 nM	0.034 nM	120 min	This work

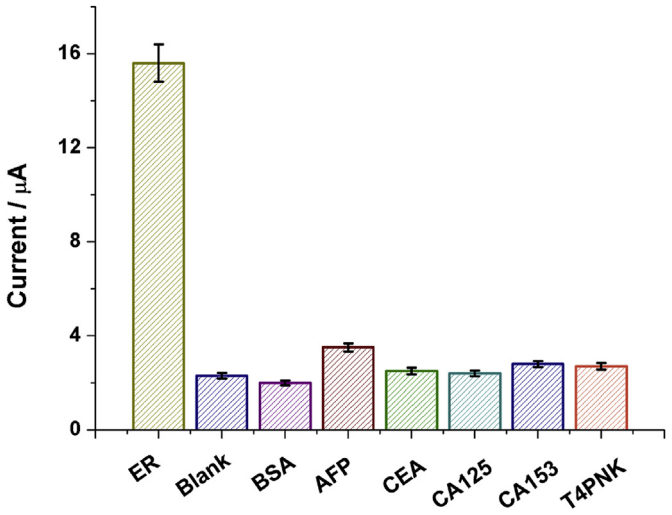

Fig. 4. Selectivity of the biosensor. Comparison of the DPV peak currents in the presence of BSA, AFP, CEA, CA125, CA153, T4PNK and ER, respectively, in which the blank was PBS buffer. The concentrations of ER and interfering proteins are about 1 nM and 5 nM respectively. The error bars were the standard deviations from three independent experiments.

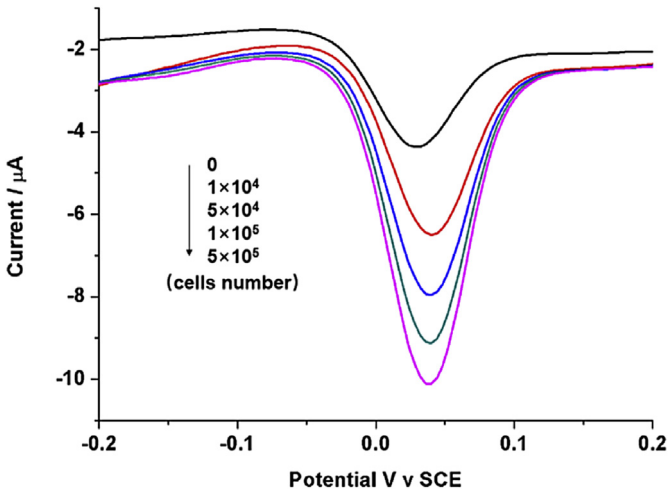

Fig. 5. DPVs obtained in detecting MCF-7 cells (1×10^4, 5×10^4, 1×10^5, and 5×10^5 cells).

obtained only for the samples containing the target ER. While the changes of signals for interfering proteins are negligible. These results showed the biosensor had an excellent specificity due to the highly specific interaction between the dsDNA probe and ER.

3.7. Detection of ER in cells

It is important to assess the applicability of the proposed biosensor for ER detection in tumor cells. So, we detected the ER in MCF-7 cell line. As shown in Fig. 5, an DPV response was evident in MCF-7 cell line. Moreover, the DPV peaks increased along with the number of cells, indicating the capability of the biosensor for monitoring ER level in cells.

4. Conclusions

In summary, we successfully fabricated a label-free biosensor for amplified detection of ER using a DNA Y junction mediated DNA HRP-mimicking DNAzyme for signal transduction. The signal amplification efficiency of HRP-mimicking DNAzyme can be realized due to target protein protection strategy. As a result, an enhanced electrochemical signal for ultrasensitive detection of ER down to 0.034 nM was obtained. Meanwhile, the biosensor can be applied to reliable monitoring of ER in cancer cells. The proposed strategy is simple without complex labeling and immobilization procedures or separation steps, making this DNA-Y junction sensing system particularly suitable for routine monitoring of ER in environmental and biological samples. It may have a great potential application in diagnosis of cancer.

Funding

This work was supported by the National Natural Science Foundation of China (Grant No. 81703088), and the Medical Research Project of Jiangsu Provincial Health and Family Planning Commission, China (Grant No. H2018113).

Conflicts of interest

The authors declare no conflict of interest.

Declaration of competing interest

The authors declare that they have no known competing financial interests or personal relationships that could have appeared to influence the work reported in this paper.

Acknowledgments

We thank professor Tao Gao (Nanjing Normal University) for providing language help in this study.

Appendix A. Supplementary data

Supplementary data to this article can be found online at https://doi.org/10.1016/j.aca.2019.08.028.

References

[1] E.R. Levin, Plasma membrane estrogen receptors, Trends Endocrinol. Metab. 20 (2009) 477–482.
[2] T.C. Guillette, T.W. Jackson, S.M. Belcher, Duality of estrogen receptor β action in cancer progression, Curr. Opin. Pharmacol. 41 (2018) 66–73.
[3] C.F. Tsai, Y.K. Cheng, D.Y. Lu, S.L. Wang, C.N. Chang, P.C. Chang, W.L. Yeh, Inhibition of estrogen receptor reduces connexin 43 expression in breast cancers, Toxicol. Appl. Pharmacol. 338 (2018) 182–190.
[4] T. Luo, J.K. Kim, The role of estrogen and estrogen receptors on cardiomyocytes: an overview, Can. J. Cardiol. 32 (2016) 1017–1025.
[5] C. Wang, F. Bai, L.H. Zhang, A. Scott, E. Li, X.H. Pei, Estrogen promotes estrogen

receptor negative BRCA1-deficient tumor initiation and progression, Breast Canc. Res. 20 (2018) 74.
[6] C. Thomas, J.Å. Gustafsson, Estrogen receptor mutations and functional consequences for breast cancer, Trends Endocrinol. Metab. 26 (2015) 467.
[7] D. Basile, M. Cinausero, D. Iacono, G. Pelizzari, M. Bonotto, M.G. Vitale, L. Gerratana, F. Puglisi, Androgen receptor in estrogen receptor positive breast cancer: beyond expression, Cancer Treat Rev. 61 (2017) 15–22.
[8] P.A. Gehrig, L. Van Le, B. Olatidoye, J. Geradts, Estrogen receptor status, determined by immunohistochemistry, as a predictor of the recurrence of stage I endometrial carcinoma, Cancer 86 (1999) 2083–2089.
[9] C.F. Sun, T.L. Wu, K.C. Tsao, J.T. Wu, Development of two ELISA for estrogen and progesterone receptor with sufficient sensitivity for fine needle aspirate and core biopsy, J. Clin. Lab. Anal. 15 (2001) 138–143.
[10] V.V. Chaban, A.J. Lakhter, P. Micevych, A membrane estrogen receptor mediates intracellular calcium release in astrocytes, Endocrinology 145 (2004) 3788–3795.
[11] R. Ahirwar, A. Dalal, J.G. Sharma, B.K. Yadav, P. Nahar, A. Kumar, S. Kumar, An aptasensor for rapid and sensitive detection of estrogen receptor alpha in human breast cancer, Biotechnol. Bioeng. 116 (2019) 227–233.
[12] S. Zhu, Y. Cao, Y. Xu, Y. Yin, G. Li, An exonuclease III protection-based electrochemical method for estrogen receptor assay, Int. J. Mol. Sci. 14 (2013) 10298–10306.
[13] L. Yu, H. Xu, H. Chen, S. Zhang, T. Jiang, L. Bai, W. Wang, S. Gao, J. Jin, Label-free DNA Y junction for detection of Hg2+ using exonuclease III or graphene oxide-assisted background reduction, Microchem. J. 145 (2019) 1086–1093.
[14] Y. Huang, W. Wang, T. Wu, L.-P. Xu, Y. Wen, X. Zhang, A three-line lateral flow biosensor for logic detection of microRNA based on Y-shaped junction DNA and target recycling amplification, Anal. Bioanal. Chem. 408 (2016) 8195–8202.
[15] X. Dong, W. Zhao, G. Sun, J. Xu, H. Chen, An electrochemical DNA biosensor based on gold nanofilm and stable Y junction structure, Acta Chim. Sin. 70 (2012) 1457–1463.
[16] L. Niu, X. Yang, W. Pan, T. Zhou, D. Liu, C. Mao, D. Liang, Effects of structural flexibility on the kinetics of DNA Y-junction assembly and gelation, Langmuir 32 (2016) 12862–12868.
[17] W. Liu, C. Gan, W. Chang, A. Qileng, H. Lei, Y. Liu, Double-integrated mimic enzymes for the visual screening of Microcystin-LR: copper hydroxide nanozyme and G-quadruplex/hemin DNAzyme, Anal. Chim. Acta 1054 (2019) 128–136.
[18] S. Liu, J. Ding, W. Qin, Dual-analyte chronopotentiometric aptasensing platform based on a G-quadruplex/hemin DNAzyme and logic gate operations, Anal. Chem. 91 (2019) 3170–3176.
[19] L. Wang, Y. Wen, L. Li, X. Yang, N. Jia, W. Li, J. Meng, M. Duan, X. Sun, G. Liu, Sensitive and label-free electrochemical lead ion biosensor based on a DNAzyme triggered G-quadruplex/hemin conformation, Biosens. Bioelectron. 115 (2018) 91–96.
[20] J. Li, G. He, B. Wang, L. Shi, T. Gao, G. Li, Fabrication of reusable electrochemical biosensor and its application for the assay of alpha-glucosidase activity, Anal. Chim. Acta 1026 (2018) 140–146.
[21] H. Li, J. Chang, T. Hou, F. Li, HRP-mimicking DNAzyme-catalyzed in situ generation of polyaniline to assist signal amplification for ultrasensitive surface plasmon resonance biosensing, Anal. Chem. 89 (2017) 673–680.
[22] Z. Zhou, L. Peng, X. Wang, Y. Xiang, A. Tong, A new colorimetric strategy for monitoring caspase 3 activity by HRP-mimicking DNAzyme-peptide conjugates, Analyst 139 (2014) 1178–1183.
[23] Y. Yuan, R. Yuan, Y. Chai, Y. Zhuo, X. Ye, X. Gan, L. Bai, Hemin/G-quadruplex simultaneously acts as NADH oxidase and HRP-mimicking DNAzyme for simple, sensitive pseudobienzyme electrochemical detection of thrombin, Chem. Commun. 48 (2012) 4621–4623.
[24] X. Mao, G. Chen, Z. Wang, Y. Zhang, X. Zhu, G. Li, Surface-immobilized and self-shaped DNA hydrogels and their application in biosensing, Chem. Sci. 9 (2018) 811–818.
[25] K. Lozano Untiveros, E.G. da Silva, F.C. de Abreu, E.F. da Silva-Junior, J.X. de Araujo-Junior, T. Mendoca de Aquino, S.M. Armas, R.O. de Moura, F.J.B. Mendonca-Junior, V.L. Serafim, K. Chumbimuni-Torres, An electrochemical biosensor based on Hairpin-DNA modified gold electrode for detection of DNA damage by a hybrid cancer drug intercalation, Biosens. Bioelectron. 133 (2019) 160–168.
[26] X. Wang, Y. Liu, J. Zhang, G. Li, Oxime chemistry-mediated covalent capturing on electrode surface with guanidinium recognition and application for aldolase activity assay, Sens. Actuators B Chem. 242 (2017) 687–693.
[27] C. Li, Y. Tao, Y. Yang, Y. Xiang, G. Li, In vitro analysis of DNA-protein interactions in gene transcription using DNAzyme-based electrochemical assay, Anal. Chem. 89 (2017) 5003–5007.
[28] J. Li, B. Wang, S. Gu, Y. Yang, Z. Wang, Y. Xiang, Amperometric low potential aptasensor for the fucosylated Golgi protein 73, a marker for hepatocellular carcinoma, Microchimica Acta 184 (2017) 3131–3136.
[29] J. Zheng, T. Gao, H. Shi, Y. Huang, Y. Xiang, G. Li, Electrochemical analysis of 8-hydroxy-2'-deoxyguanosine with enhanced sensitivity based on exonuclease-mediated functional nucleic acid, Talanta 199 (2019) 324–328.
[30] Q. Xiao, J. Feng, M. Feng, J. Li, Y. Liu, D. Wang, S. Huang, A ratiometric electrochemical aptasensor for ultrasensitive determination of adenosine triphosphate via a triple-helix molecular switch, Microchimica Acta 186 (2019).